GENERAL INSTRUCTIONS

- **Authors: Carefully check the page proofs (and coordinate with all authors); additional changes or updates WILL NOT be accepted after the article is published online/print in its final form. Please check author names and affiliations, funding, as well as the overall article for any errors prior to sending in your author proof corrections. Your article has been peer reviewed, accepted as final, and sent in to IEEE. No text changes have been made to the main part of the article as dictated by the editorial level of service for your publication.**
- **Authors: When accessing and uploading your corrections at the Author Gateway, please note we cannot accept new source files as corrections for your article. Do not send new Latex, Word, or PDF files, as we cannot simply "overwrite" your article. Please submit your corrections as an annotated PDF or as clearly written list of corrections, with location in article, using line numbers provided on your proof. You can also upload revised graphics to the Gateway.**
- **Authors: Please note that once you click "approve with no changes," the proofing process is now complete and your article will be sent for final publication and printing. Once your article is posted on Xplore, it is considered final and the article of record. No further changes will be allowed at this point so please ensure scrutiny of your final proof.**
- **Authors: Unless invited or otherwise informed, overlength page charges of $260 per page are mandatory for each page in excess of seven printed pages and are required for publication. If you have any questions regarding overlength page charges, need an invoice, or have any other billing questions, please contact reprints@ieee.org as they handle these billing requests.**

QUERIES

Q1. Author: Please confirm or add details for any funding or financial support for the research of this article.
Q2. Author: Please provide the postal codes in the affiliaitons.
Q3. Author: Please provide the translation version for Ref. [9]. Also, the complete page range.
Q4. Author: Please check and confirm whether the educational qualification of authors Anton V. Dyshlyuk and Oleg B. Vitrik are correct as set.

Tunable Autler-Townes-Like Resonance Splitting in a Bent Fiber-Optic Fabry-Perot Resonator: 3D Modeling and Experimental Verification

Anton V. Dyshlyuk, Uliana A. Eryusheva, and Oleg B. Vitrik

***Abstract*—We present a numerical and experimental study of resonance splitting in the transmission and reflection spectra of the Fabry–Perot resonator made of a bent section of a conventional single-mode optical fiber with metallized end faces. We show the splitting to be similar in nature to the well-known Autler–Townes effect and to arise from the strong coupling between the core mode and cladding whispering gallery mode of the bent fiber. The effect of all major parameters of the bent resonator on the splitting of its resonances is demonstrated. Potential applications of the observed effects in the field of precision optical refractometry as well as further research directions are discussed.**

***Index Terms*—Autler-Townes splitting, electromagnetically induced transparency, Fano resonance, optical fiber bend, optical refractometry.**

I. Introduction

FANO resonances and related phenomena, similar to electromagnetically-induced transparency and Autler-Townes (Rabi) splitting, attract considerable attention of researchers in photonics, nanooptics, plasmonics and metamaterials due to the intriguing possibilities of tailoring the frequency response of resonant systems [1]–[7]. For example, an asymmetric Fano line shape or a narrow dip in a wide resonance, characteristic of electromagnetic-induced transparency, can provide an extremely sharp drop from maximum to almost zero in the reflection, transmission, extinction, scattering spectra, etc. This is a very attractive feature for the design of functional elements of photonics, especially switching and sensing devices.

In [8], [9] we have for the first time, to the best of our knowledge, demonstrated and studied tunable Fano resonances and related effects observed in a Fabry-Perot resonator made up of a bent slab single-mode waveguide with metallized ends. The discovered effects may find diverse applications, with one of the more obvious among them dealing with precision optical refractometry. Several designs of refractive index (RI) sensors based on bent single-mode optical fibers (OF) have already been reported, which use strong coupling between freely propagating fundamental and cladding modes [10]–[13]. In terms of their simple optical layout such fiber optic refractometers compare favorably with analogs, the latter typically requiring chemical (etching) or mechanical (polishing) processing of the fiber or additional elements such as long-period or tilted waveguide diffraction gratings [14]. However, in terms of metrological performance, they are typically inferior to more traditional refractometric techniques, for example, based on the well-known Kretschman scheme [15], [16]. The Fano resonances and related effects demonstrated in [8], [9] open up a new degree of freedom in the design of bent fiber based photonic devices and can provide a significant improvement in the measurement performance of the bent fiber-based RI sensors thus leading to the development of novel compact, portable, and inexpensive ultra-sensitive fiber-optic refractometers, for example, for bio- and chemosensing applications. In [8], [9], however, we have studied these phenomena only numerically and in a simplified 2D geometry. The present work, which is a follow-up research on the same topic, is aimed at a rigorous modeling of these effects in the full three-dimensional geometry of a bent optical fiber with circular cross-section and their experimental demonstration using conventional telecom single-mode optical fibers.

We must emphasize that although we deal here with a Fabry-Perot resonator, the particular type of the resonator is not essential. Similar results can be obtained with a ring or some other kind of a resonator based on the bent optical fiber. The key point that we want to make with this and our preceding work is twofold. Firstly, we wish to demonstrate how, by introducing a longitudinal resonator, one can bridge the gap between bent fiber-based photonic devices and the physics behind Fano resonances, electromagnetically induced transparency and Autler-Townes splitting. This opens up a new dimension in the design of functional elements of photonics and may lead to applications far beyond those that we currently anticipate. Secondly, we wish to show that a bent single mode fiber-based resonator already consists, effectively, of two coupled resonators. This enables one to obtain a full range of Fano-like resonant features without

Manuscript received May 19, 2020; revised July 13, 2020; accepted July 26, 2020. This work was supported by the Russian Foundation for Basic Research under Grant 20-02-00556A. *(Corresponding author: Anton V. Dyshlyuk.)*

Anton V. Dyshlyuk is with the Institute of Automation and Control Processes (IACP) FEB RAS, Far Eastern Federal University (FEFU) and Vladivostok State University of Economics and Service (VSUES), Vladivostok, Russia (e-mail: anton_dys@iacp.dvo.ru).

~~UlianaA.~~ Eryusheva is on leave from the Institute of Automation and Control Processes (IACP) FEB RAS Vladivostok, Russia (e-mail: muzika.com@inbox.ru).

Oleg B. Vitrik is with the Institute of Automation and Control Processes (IACP) FEB RAS, Far Eastern Federal University (FEFU), Vladivostok, Russia (e-mail: oleg_vitrik@mail.ru).

Color versions of one or more of the figures in this article are available online at https://ieeexplore.ieee.org.

Digital Object Identifier 10.1109/JLT.2020.3021122

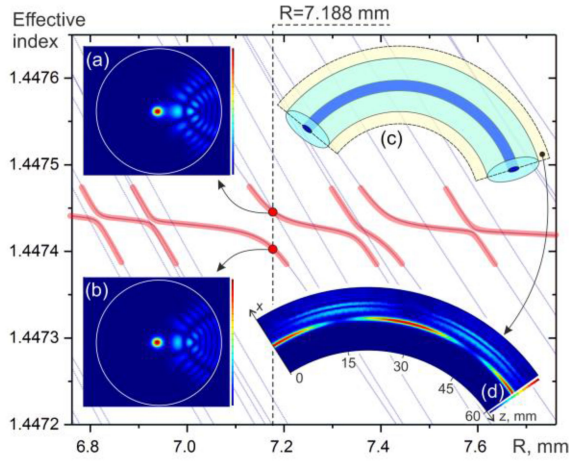

Fig. 1. Effective indexes of the bent single-mode optical fiber supermodes vs. bend radius at a fixed wavelength of 1550 nm. In the insets: (a), (b) amplitude profiles of the two supermodes at the radius of a pronounced anti-crossing of their dispersion curves (R = 7.188 mm), (c) schematic drawing of the bent single-mode optical fiber (shown in pale yellow is the symmetry plane), (d) electric field amplitude distribution of guided light in the longitudinal section of the bent optical fiber at R = 7.188 mm.

the need for designing two separate coupled resonators (such as coupled ring resonators) or using additional scattering elements (such as FBG) to introduce coupling between different resonant states in a single resonator.

The paper is organized as follows. First, based on the analysis of mode coupling in a bent naked single-mode OF, tunable resonance line splitting in the reflection and transmission spectra of a bent Fabry-Perot fiber-optic resonator will be demonstrated, similar to the well-known Autler-Townes splitting. Then, the effect of all major geometric parameters of the bent resonator on the observed splitting will be demonstrated and discussed. In the final part of the article we will present the experimental results, make their comparison with the results of numerical modeling, and discus further research directions.

II. Numerical Results and Discussion

The bent single-mode SMF-28-type optical fiber under study is shown schematically in Fig. 1(c) and has the following parameters: core radius $\rho_1 = 4.15$ μm, core refractive index $n_1 = 1.4504$, optical cladding radius $\rho_2 = 62.5$ μm, cladding refractive index $n_2 = 1.4447$, and bend radius R. To model propagation of guided light in the fiber we use bidirectional eigenmode expansion method implemented in the Lumerical MODE Solutions software. Throughout the simulations we assume that the polymer coatings have been removed from the fiber so that its quartz optical cladding is in contact with air with RI $n_3 = 1$. Therefore, due to the total internal reflection at the cladding | air interface, not only the core, but also the cladding of the fiber possesses pronounced light-guiding properties. Moreover, due to the large discontinuity in refractive index at the cladding | ambient medium interface, the loss of guided light through tunneling out of the bent fiber is negligible (at the bend radii considered in the work), so that all the modes of the fiber, including cladding modes can, to a good approximation, be considered guided modes with zero propagation losses, with their field confined to the fiber. For this reason, to simplify numerical modeling we disregard radiation modes and use reflecting, rather than absorbing, boundary conditions of the type perfect electric conductor (PEC) at the external boundaries of the calculation domain.

Generally speaking, there are two basic lines of reasoning about light propagation through the bent fiber under study [17]. Within the first appoximate approach, its core and cladding are considered separately: the core supports a single fundamental mode (FM), whereas the cladding - a large number of cladding modes. As a result of bending, the field of the cladding modes shifts along the bend radius so that they are guided predominantly by that outer (with respect to the bend) surface of the cladding, which effectively turns them into whispering gallery modes (WGMs). With certain combinations of wavelength and bend radius, the effective refractive indices of FM and a WGM become equal, which leads to the strong coupling between them. The coupled modes then exchange power as they propagate along the fiber, which is observed as periodic redistribution of guided light intensity between the core and the cladding of the fiber (Fig. 1(d)). The period of this exchange depends on the coupling coefficient determined by the overlap integral of the FM and WGM profiles, and decreases with the growth of the latter [17].

In the second more exact approach, the modes of the entire bent fiber viewed as a whole are calculated, which are hereinafter referred to as supermodes. If no coupling takes place between the FM and WGM, the supermodes, in terms of their effective indexes and profiles, do not differ much from the corresponding modes considered separately. However, when such a coupling does occur, the dispersion curves of supermodes, in contrast to those of FM and WGMs, exhibit a characteristic anti-crossing behavior, which is a well-known signature of the strong coupling regime [18]. This is illustrated in Fig. 1, which shows the effective indexes of bent fiber supermodes vs bend radius at a fixed wavelength of 1550 nm. Within an anti-crossing, the amplitude profiles of both supermodes, as Fig. 1a and 1(b) show, are similar and represent a superposition of the separately considered FM (local maximum in the region of the core) and WGM (field distribution in the cladding to the right of the core) profiles, i.e. they result from the hybridization of the latter. The phase profiles of the supermodes, however, are quite different so that the redistribution of guided light intensity between the core and cladding of the bent fiber corresponds to the interference (beating) of the supermodes as they propagate along the bent fiber with constant amplitudes (in contrast to the separately considered FM and WGM whose amplitudes vary as functions of the coordinate along the bent fiber's optical axis as a result of the coupling). The beating period is given by $\lambda / \Delta n$, where Δn is the difference of the effective indexes of the supermodes at the anti-crossing of their dispersion curves, which, in terms of the separately considered FM and WGM, is determined by their coupling coefficient.

The exchange of power between the coupled FM and WGM has a clear parallel to a simple mechanical system of two coupled pendulums (Fig. 2(b)). In the free oscillation regime, the growth

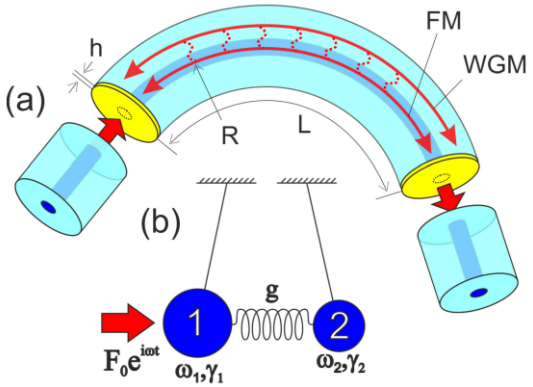

Fig. 2. Schematic of the bent fiber optic Faby-Perot resonator (a) and its mechanical analogy (b)

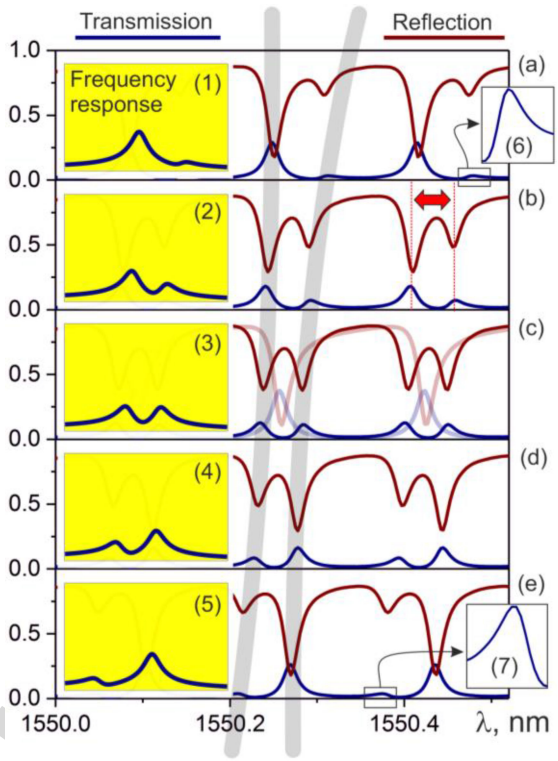

Fig. 3. The calculated reflection and transmission spectra of the bent fiber-optic Fabry-Perot resonator at L = 5mm, h = 10 nm and R = 7.15 mm (a); R = 7.175 mm (b); R = 7.188 mm (c); R = 7.2 mm (d); R = 7.225 (e). In Fig. 3 (c), for comparison, the reflection and transmission spectra of the corresponding straight resonator (L = 5 mm, h = 10 nm) are shown with semi-transparent lines. The insets on the left show the frequency response of the driven pendulum 1 in the mechanical system, calculated for $\omega_1 = 1$, $\gamma_1 = \gamma_2 = 0.1$, g = 0.2, and $\omega_2 = 1.2$ (1) ; $\omega_2 = 1.05$ (2); $\omega_2 = 0.98$ (3); $\omega_2 = 0.9$ (4); $\omega_2 = 0.75$ (5). The insets (6) and (7) show an enlarged view of the secondary peak in the transmission spectrum of the bent FPR with an asymmetric Fano line shape. The gray vertical semi-transparent lines illustrate the shift of the split resonance lines with changing of the bend radius.

in oscillation amplitude of one of them is accompanied by the decrease of that of the other [19], i.e. their motion in time is analogous to the spatial variation of the amplitudes of the coupled FM and WGM in the bent fiber (Fig.1(d)).

It is well known that in mechanical systems of coupled oscillators one can readily observe Fano resonances as well as effects similar to the Autler-Townes splitting but in the forced, rather than free, oscillation regime under the action of a harmonic driving force applied to one of the pendulums [7], [18]. At a sufficiently high coupling coefficient the resonance peak in the frequency response of the driven oscillator splits and, depending of the resonant frequency of the other oscillator, one can obtain either symmetric splitting pattern characteristic of the Aulter-Townes effect, or asymmetric splitting with a pronounced dominant peak and weak secondary peak with an asymmetric line shape (insets 1-5 in Fig. 3(a)-(d)).

To realize a similar oscillation regime in the optical domain using a bent single-mode optical fiber let us form a Fabry-Perot resonator (FPR) by applying gold mirrors of thickness h to the end faces of a section of bent fiber of length L as shown in Fig. 2a. Light is fed into and output from the resonator through straight input and output section of the same fiber. Such a resonator can be viewed as two separate coupled resonators corresponding to the longitudinal resonances of the coupled fundamental (FM-resonator) and whispering gallery (WGM-resonator) modes. The excitation light guided by the core of the input fiber section and fed into the core of the bent resonator through the left mirror plays the same role as the driving force applied to one of the pendulums in the mechanical system (Fig. 2(b)).

We plot in Fig. 3 the numerically calculated reflection and transmission spectra of the bent FPR for various bend radii near R = 7.188 mm where a pronounced anti-crossing is observed in the dispersion curves of the supermodes of the bent optical fiber (Fig. 1).

For the sake of comparison, we also show with semi-transparent lines in Fig. 3(c) the reflection and transmission spectra of the corresponding straight resonator. The reflection and transmission coefficients are defined, respectively, as the ratio of powers of the reflected FM in the input fiber section and transmitted FM in the output section to the power supplied by the exciting fundamental mode in the input section.

As seen from the comparison of the straight and bent RFP spectra in Fig. 3c, the bending of the resonator brings about splitting of the resonances, which at R = 7.188 mm is symmetric and similar to the Autler-Townes splitting. Increasing or decreasing the bend radius relative to R = 7.188 mm shifts the split resonance lines in a manner shown schematically with grey vertical semi-transparent lines. Obviously, the pattern of this shifting is defined by the anti-crossing behavior of the dispersion curves of the bent fiber supermodes (Fig. 1). Furthermore, as the bend radius departs from the resonant value of 7.188 mm the secondary peak in the transmission spectrum and the corresponding dip in the reflection spectrum become less pronounced, which makes the splitting less appreciable.

We also note that at R = 7.15 mm and R = 7.225 mm the weak secondary transmission peak has an asymmetric line shape characteristic of a low Q-factor Fano resonance (insets 6 and 7 in Fig. 3(a), 3(e)).

To interpret the obtained results, it is worthwhile to compare the transmission spectrum of the bent fiber optic resonator with the frequency response of the driven pendulum in the mechanical oscillatory system (insets 1-5 in Fig. 3(a)-(e)). Clearly,

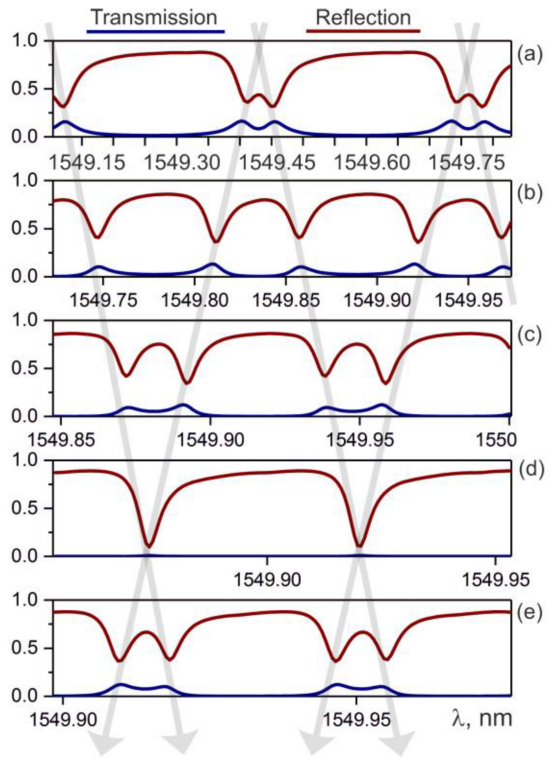

Fig. 4. The calculated transmission and reflection spectra of a bent Fabry-Perot fiber-optic resonator at R = 7.188 mm, h = 10 nm and L = 2.5 mm (a); L = 7.5 mm (b); L = 12.5 mm (c); L = 18 mm (d); L = 22.5 mm (e). The gray vertical lines schematically illustrate the displacement of the split resonance lines as the length of the resonator changes.

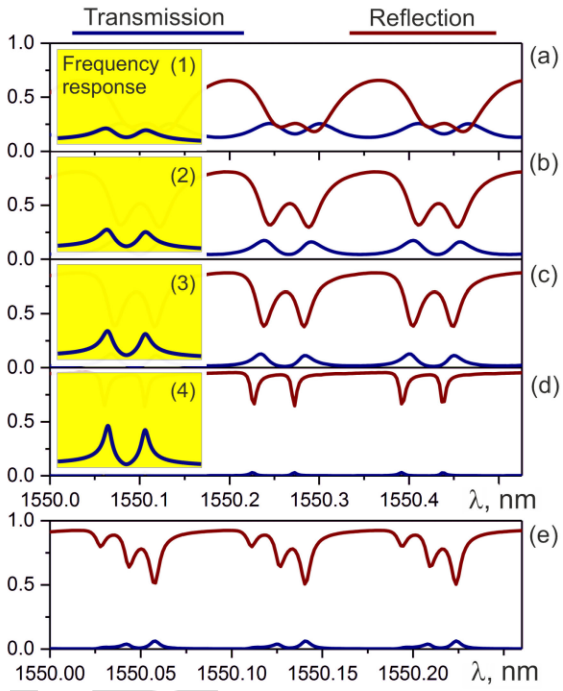

Fig. 5. The calculated transmission and reflection spectra of a bent Fabry-Perot fiber-optic resonator at R = 7.188 mm, L = 5 mm and various mirror thicknesses: h = 5 nm (a); h = 7.5 nm (b); h = 10 nm (c); h = 22.5 nm (d). The insets on the left show the frequency response of the driven pendulum 1 in the mechanical oscillatory system, calculated for $\omega_1 = 1$, $\omega_2 = 0.98$, g = 0.2 and $\gamma_1 = \gamma_2 = 0.15$ (1); 0.1 (2); 0.075 (3); 0.05 (4). Figure (e) shows an example of irregular splitting of the bend FPR resonances when the fundamental mode is coupled simultaneously to two WGMs (R = 7.375 mm, L = 10 mm, h = 15 nm).

these spectra are virtually identical, which is an evidence of a close analogy between the mechanical and optical systems under consideration. In terms of this analogy, the FM-resonator corresponds to the driven pendulum 1, whereas WGM-resonator – to the coupled pendulum 2 (Fig. 2(b)). The coupling between fundamental and whispering gallery modes in the bent fiber then plays the role of the coupling spring in the mechanical system.

As a result of the strong dependence of WGM effective index on the bend radius, the resonances of the WGM-resonator shift with changing R, whereas the resonant frequencies of the FM-resonator remain nearly constant. Changing the bend radius is thus equivalent to varying the second pendulum's resonant frequency (ω_2) while keeping that of the first one (ω_1) fixed in the mechanical system. R = 7.188 mm corresponds to the phase matching condition between FM and WGM in the bent fiber, which makes the resonant frequencies of the FM- and WGM-resonators match each other. This case, therefore, corresponds to $\omega_1 \approx \omega_2$ in the mechanical system when a clear-cut symmetric resonance splitting is observed. As the bend radius departs from 7,188 mm the phase matching between FM and WGM is gradually lost making the splitting asymmetric and less pronounced, which in terms of the mechanical system corresponds to $\omega_1 \lessgtr \omega_2$.

To demonstrate the effect of the FPR length on the resonance splitting, we plot in Fig. 4 its transmission and reflection spectra calculated at L = 2.5 …22.5 mm, R = 7.188 mm, and h = 10 nm. As seen from the figure, increasing the length of the resonator makes the splitting look more pronounced by driving the split resonance lines further apart. This, however, is an apparent effect arising from different scales on the horizontal axes of Fig. 4(a)-(e). A closer analysis of the presented spectra shows that an increase in the length of the resonator makes its lines sharper and more closely spaced while the splitting remains unchanged in its absolute value.

An interesting feature is observed at L = 18 mm (Fig. 4(d)) when the resonant transmission is almost zeroed by the overlap of the split lines from two adjacent resonances, which is accompanied by a deep minimum in the reflection spectrum. The calculation of the intensity distribution in the bent resonator shows that almost all of the injected power goes, in this case, into the cladding of the output fiber section.

Figure 5 illustrates the effect of the mirror thickness on the resonance splitting of the bent FPR by showing its transmission and reflection spectra calculated at h = 5; 7.5; 10 and 22.5 nm; R = 7.188 mm, L = 5 mm. As seen from the graphs, the primary effect of thicker mirrors is to make the resonance lines sharper as a result of higher mirror reflectivity and, therefore, higher Q-factor of the resonator. Narrowing of the resonance lines, in turn, makes their splitting more clear-cut. Disregarding the lowering of the resonant transmission with an increase in *h*, which results from higher absorption losses in thicker mirrors, the calculated transmission spectra, as seen from insets 1-4, are

very similar to the frequency response of the driven pendulum in the mechanical system (Fig. 2(b)) with simultaneously decreasing both pendulums' damping constants γ_1 and γ_2.

All the results shown above are obtained for the bend radii near the resonant value of R = 7.188 mm, which corresponds to the strong coupling of the fundamental mode of the core to one of the cladding whispering gallery modes. There are, however, a great number of such cladding modes many of which can couple to FM at various R values, as can be readily appreciated from Fig. 1. The splitting of resonances similar to that already demonstrated can therefore be observed at different bend radii. Its width is defined by the effective index difference of the hybrid supermodes of the bent fiber at the anti-crossing of their dispersion curves, Δn.

In terms of the separately considered FM and WGM, Δn is determined by their coupling coefficient and is therefore a measure of the coupling strength of FM- and WFM-resonators. As seen from Fig. 1, in the bend radius range from 6.8 to 7.7 mm Δn is largest for the anti-crossing centered at R = 7.188 mm. At the bend radii of other anti-crossings, the width of the splitting will be less, meaning that larger Q-factors of the resonator are required to observe it clearly.

We also note that around certain bend radii the fundamental mode may become coupled to two WGMs simultaneously (Fig. 1). This leads to a more complicated and irregular splitting pattern in the transmission and reflection spectra of the bent FPR, as exemplified by Fig. 5(e).

All the simulation results in this article are obtained for the case when the FM in the input fiber section is polarized linearly in the plane of the fiber bend, which corresponds to the symmetric boundary condition on the symmetry plane of the structure under study (Fig. 1(c)). Calculations for the orthogonal polarization yield similar results albeit slightly shifted in wavelength due to the polarization dependence of WGMs effective indexes.

III. Experiment

A schematic of the experimental setup for the study of the resonance splitting of the bent fiber optic Fabry-Perot resonator, along with the experimental results are shown in Fig. 6.To measure experimentally the reflection spectra of the bent fiber optic Fabry-Perot resonator we prepared several samples of such resonators of 1 cm-long sections of an SMF-28-type telecom optical fiber. The end faces of the resonators are coated with a thin layer of gold by the electron beam evaporation technique in the ADVAVAC vacuum chamber. We then fix the resonators upon rounded support 7 (Fig. 6(a)) and lead-in fiber 3 is aligned with the input end of the resonator using optical microscopes, broadband light source 1 (Thorlabs ASE730) and optical spectrum analyzer 8 (Yokogawa AQ6370B). After alignment the contact point is secured with epoxy adhesive 4. Excitation of the resonator and the measurement of its reflection spectrum is carried out via fiber optic circulator 2.

The resonator is bent by calibrated displacement of its loose end using a precision translation stage 6. The evolution of the bent resonator's measured reflection spectrum with varying bend radius is illustrated in Fig. 6(b)-(f). The insets 1-5 of these figures show the corresponding simulation results. Obviously,

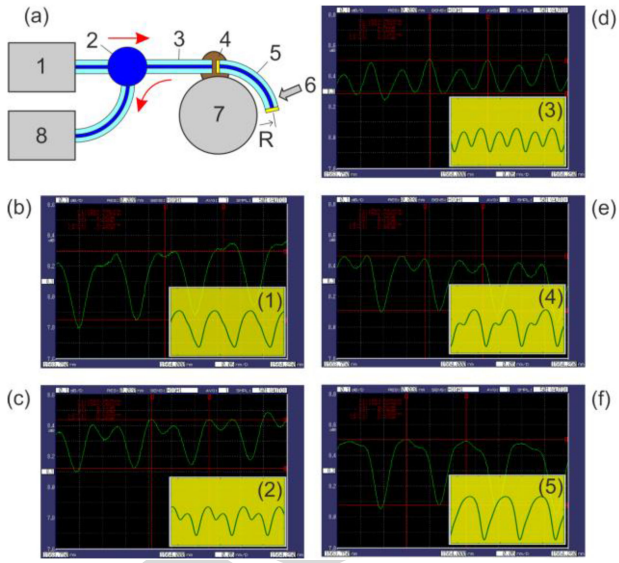

Fig. 6. Schematic representation of the experimental setup for studying the reflection spectrum of a bent fiber optic Fabry-Perot resonator (a): 1 - broadband light source (Thorlabs ASE 730), 2 - fiber-optic circulator , 3 – exciting optical fiber, 4 - fixing the contact point with an epoxy adhesive, 5 – bent fiber optic Fabry-Perot resonator, 6 - bending the resonator by calibrated displacement of its loose end using a precision translation stage , 7 – a rounded support, 8 - optical spectrum analyzer (Yokogawa AQ6370B). The evolution of the measured reflection spectra with varying bend radius (b)-(f). Yellow insets (1-5) show the corresponding numerically calculated reflection spectra at L = 1 cm, h = 5 nm and R = 7.375 mm (1), R = 7.4 mm (2), R = 7.425 mm (3), R = 7.45 mm (4), R = 7.475 mm (5).

the experimental and numerical results are in good agreement, which confirms the validity of the numerical modeling carried out in this work.

IV. Conclusions

We have, thus, studied tunable splitting of resonances in the transmission and reflection spectra of the bent single mode optical fiber-based Fabry-Perot resonator, which is similar to the well-knows Autler-Townes splitting. The splitting is shown to result from the strong coupling between the fundamental mode of the core and whispering gallery modes of the cladding of the bent fiber. We have demonstrated and discussed how the splitting is affected by all major parameters of the resonator. The validity of the numerical modeling is confirmed by the experimental results.

We must note that the resonance splitting demonstrated in this work does not lead to narrow spectral features and sharp drops in the transmission and reflection spectra, characteristic of high Q-factor Fano resonances and electromagnetically induced transparency. This is due to the fact that the latter effects arise from the interference of a narrow resonant lineshape with a nonresonant continuum or another low Q-factor resonance. In particular, to observe such effects in the mechanical system of two coupled pendulums (Fig. 2(b)) the following condition must be satisfied: $\gamma_2 << \gamma_1$ [7]. In the studied case of coupling between FM- and WGM-resonators, however, their losses, defined primarily by the transmission through the input and output mirrors, are equal. To enable high Q-factor Fano

resonance and electromagnetically induced transparency-like operation regimes in the bent fiber optic Fabry-Perot resonator, which are more attractive in terms of the ~~development fiber,~~ optic sensing and switching devices, variable transmission mirrors must be employed providing low losses for the WGM-resonator and high losses for the FM-resonator. The simplest example of such a mirror is a thick gold layer on the fiber end face with a hole at the center produced by a laser ablation technique. Results of further researches in this direction will be published elsewhere.

We stress again that although we have studied here the Fabry-Perot resonator, the particular type of resonator is not essential and similar results can be obtained with other kinds of bent fiber-based resonators. The most important point we wish to make is that, by introducing a longitudinal resonator, one can obtain a full range of Fano-like resonant features with a single section of conventional bent single-mode optical fiber without resorting to any additional coupling elements or building a system of two separate coupled resonators. This opens up a new degree of freedom in the design of functional elements of photonics based on bent optical fibers and waveguides and may lead to diverse applications far beyond what we currently anticipate.

REFERENCES

[1] U. Fano, "Sullo spettro di assorbimento dei gas nobili presso il limite dello spettro darco," *Il Nuovo Cimento*, vol. 12, pp. 154–161, 1935.

[2] U. Fano, "Effects of configuration interaction on intensities and phase shifts," *Phys. Rev.*, vol. 124, no. 6, 1961, Art. no. 1866.

[3] M. F. Limonov *et al.*, "Fano resonances in photonics," *Nature Photon.*, vol. 11, no. 9, 2017, Art. no. 543.

[4] B. Luk'yanchuk *et al.*, "The Fano resonance in plasmonic nanostructures and metamaterials, *Nature Mater.*, vol. 9, no. 9, 2010, Art. no. 707.

[5] A. E. Miroshnichenko, S. Flach, and Y. S. Kivshar, "Fano resonances in nanoscale structures," *Rev. Modern Phys.*, vol. 82, no. 3, 2010, Art. no. 2257.

[6] M. Rahmani, B. Luk'yanchuk, and M. Hong, "Fano resonance in novel plasmonic nanostructures," *Laser Photon. Rev.*, vol. 7, no. 3, pp. 329–349, 2013.

[7] C. L. Garrido Alzar, M. A. G. Martinez, and P. Nussenzveig, "Classical analog of electromagnetically induced transparency," *Amer. J. Phys.*, vol. 70, no. 1, pp. 37–41, 2002.

[8] A. V. Dyshlyuk, "Tunable Fano-like resonances in a bent single-mode waveguide-based Fabry–Perot resonator," *Opt. Lett.*, vol. 44, no. 2, pp. 231–234, 2019.

[9] А. В. Дышлюк, "Демонстрация резонансных эффектов типа расщепления Аутлера–Таунса, электромагнитно-индуцированной прозрачности и резонансов Фано в деформированном волноводном резонаторе," *Компьютерная оптика*, vol. 43, no. 1, 2019.

[10] A. V. Dyshlyuk *et al.*, "Numerical and experimental investigation of surface plasmon resonance excitation using whispering gallery modes in bent metal-clad single-mode optical fiber," *J. Lightw. Technol.*, vol. 35, no. 24, pp. 5425–5431, 2017.

[11] P. Wang *et al.*, "Macrobending single-mode fiber-based refractometer," *Appl. Opt.*, vol. 48, no. 31, pp. 6044–6049, 2009.

[12] P. Wang *et al.*, "A macrobending singlemode fiber refractive index sensor for low refractive index liquids," *Photon. Lett. Poland*, vol. 2, no. 2, pp. 67–69, 2010.

[13] Y. N. Kulchin, O. B. Vitrik, and S. O. Gurbatov, "Effect of small variations in the refractive index of the ambient medium on the spectrum of a bent fibre-optic Fabry–Perot interferometer," *Quantum Electron.*, vol. 41, no. 9, 2011, Art. no. 821.

[14] Y. Xu *et al.*, "Optical refractive index sensors with plasmonic and photonic structures: Promising and inconvenient truth," *Adv. Opt. Mater.*, vol. 7, no. 9, 2019, Art. no. 1801433.

[15] E. Kretschmann and H. Raether, "Radiative decay of non radiative surface plasmons excited by light," *Zeitschrift für Naturforschung A*, vol. 23, no. 12, pp. 2135–2136, 1968.

[16] J. Homola, *Surface Plasmon Resonance Based Sensors Berlin*. Berlin, Germany: Springer, 2006.

[17] A. W. Snyder and J. Love, *Optical waveguide theory*. Berlin, Germany: Springer Science & Business Media, 2012.

[18] L. Novotny, "Strong coupling, energy splitting, and level crossings: A classical perspective," *Amer. J. Phys.*, vol. 78, no. 11, pp. 1199–1202, 2010.

[19] V. Picciarelli and R. Stella, "Coupled pendulums: A physical system for laboratory investigations at upper secondary school," *Phys. Educ.*, vol. 45, no. 4, 2010, Art. no. 402.

Anton V. Dyshlyuk received the Ph.D. degree from Far Eastern State Technical University (FEFU), Vladivostok, Russia, in ~~2003, majoring in radio communications, radio broadcasting, and television.~~ He is currently a Senior Researcher with the Institute of Automation and Control Processes of FEB RAS as well as with FEFU and Vladivostok State University of Economics and Service (VSUES), Vladivostok, as a Lecturer. His research interests include fiber optics, quantum electronics, fiber optic sensors and measuring systems, biosensing, plasmonics, and nanophotonics.

Uliana A. Eryusheva received the graduate degree from the Vladivostok State University of Economics and Service, Vladivostok, Russia, in 2017 and the master's degree from Far Eastern Federal University, Vladivostok, Russia, in 2019. Her research interests include fiber optics, plasmonics, fiber optic sensors and measuring systems, and bio- and chemosensing.

Oleg B. Vitrik received the graduate degree from Moscow Engineering Physics Institute, Moscow, Russia, in 1986, majoring in solid state physics. He is currently a Principal Researcher with the Institute of Automation and Control Processes of FEB RAS and a Professor of the Far Eastern Federal University, Vladivostok, Russia. His research interests include nano-optics, plasmonics, fiber optics, fiber optic sensors, and measuring systems.

GENERAL INSTRUCTIONS

- **Authors: Carefully check the page proofs (and coordinate with all authors); additional changes or updates WILL NOT be accepted after the article is published online/print in its final form. Please check author names and affiliations, funding, as well as the overall article for any errors prior to sending in your author proof corrections. Your article has been peer reviewed, accepted as final, and sent in to IEEE. No text changes have been made to the main part of the article as dictated by the editorial level of service for your publication.**
- **Authors: When accessing and uploading your corrections at the Author Gateway, please note we cannot accept new source files as corrections for your article. Do not send new Latex, Word, or PDF files, as we cannot simply "overwrite" your article. Please submit your corrections as an annotated PDF or as clearly written list of corrections, with location in article, using line numbers provided on your proof. You can also upload revised graphics to the Gateway.**
- **Authors: Please note that once you click "approve with no changes," the proofing process is now complete and your article will be sent for final publication and printing. Once your article is posted on Xplore, it is considered final and the article of record. No further changes will be allowed at this point so please ensure scrutiny of your final proof.**
- **Authors: Unless invited or otherwise informed, overlength page charges of $260 per page are mandatory for each page in excess of seven printed pages and are required for publication. If you have any questions regarding overlength page charges, need an invoice, or have any other billing questions, please contact reprints@ieee.org as they handle these billing requests.**

QUERIES

Q1. Author: Please confirm or add details for any funding or financial support for the research of this article.
Q2. Author: Please provide the postal codes in the affiliaitons.
Q3. Author: Please provide the translation version for Ref. [9]. Also, the complete page range.
Q4. Author: Please check and confirm whether the educational qualification of authors Anton V. Dyshlyuk and Oleg B. Vitrik are correct as set.

Tunable Autler-Townes-Like Resonance Splitting in a Bent Fiber-Optic Fabry-Perot Resonator: 3D Modeling and Experimental Verification

Anton V. Dyshlyuk, Uliana A. Eryusheva, and Oleg B. Vitrik

***Abstract*—We present a numerical and experimental study of resonance splitting in the transmission and reflection spectra of the Fabry–Perot resonator made of a bent section of a conventional single-mode optical fiber with metallized end faces. We show the splitting to be similar in nature to the well-known Autler–Townes effect and to arise from the strong coupling between the core mode and cladding whispering gallery mode of the bent fiber. The effect of all major parameters of the bent resonator on the splitting of its resonances is demonstrated. Potential applications of the observed effects in the field of precision optical refractometry as well as further research directions are discussed.**

***Index Terms*—Autler-Townes splitting, electromagnetically induced transparency, Fano resonance, optical fiber bend, optical refractometry.**

I. Introduction

FANO resonances and related phenomena, similar to electromagnetically-induced transparency and Autler-Townes (Rabi) splitting, attract considerable attention of researchers in photonics, nanooptics, plasmonics and metamaterials due to the intriguing possibilities of tailoring the frequency response of resonant systems [1]–[7]. For example, an asymmetric Fano line shape or a narrow dip in a wide resonance, characteristic of electromagnetic-induced transparency, can provide an extremely sharp drop from maximum to almost zero in the reflection, transmission, extinction, scattering spectra, etc. This is a very attractive feature for the design of functional elements of photonics, especially switching and sensing devices.

In [8], [9] we have for the first time, to the best of our knowledge, demonstrated and studied tunable Fano resonances and related effects observed in a Fabry-Perot resonator made up of a bent slab single-mode waveguide with metallized ends. The discovered effects may find diverse applications, with one of the more obvious among them dealing with precision optical refractometry. Several designs of refractive index (RI) sensors based on bent single-mode optical fibers (OF) have already been reported, which use strong coupling between freely propagating fundamental and cladding modes [10]–[13]. In terms of their simple optical layout such fiber optic refractometers compare favorably with analogs, the latter typically requiring chemical (etching) or mechanical (polishing) processing of the fiber or additional elements such as long-period or tilted waveguide diffraction gratings [14]. However, in terms of metrological performance, they are typically inferior to more traditional refractometric techniques, for example, based on the well-known Kretschman scheme [15], [16]. The Fano resonances and related effects demonstrated in [8], [9] open up a new degree of freedom in the design of bent fiber based photonic devices and can provide a significant improvement in the measurement performance of the bent fiber-based RI sensors thus leading to the development of novel compact, portable, and inexpensive ultra-sensitive fiber-optic refractometers, for example, for bio- and chemosensing applications. In [8], [9], however, we have studied these phenomena only numerically and in a simplified 2D geometry. The present work, which is a follow-up research on the same topic, is aimed at a rigorous modeling of these effects in the full three-dimensional geometry of a bent optical fiber with circular cross-section and their experimental demonstration using conventional telecom single-mode optical fibers.

We must emphasize that although we deal here with a Fabry-Perot resonator, the particular type of the resonator is not essential. Similar results can be obtained with a ring or some other kind of a resonator based on the bent optical fiber. The key point that we want to make with this and our preceding work is twofold. Firstly, we wish to demonstrate how, by introducing a longitudinal resonator, one can bridge the gap between bent fiber-based photonic devices and the physics behind Fano resonances, electromagnetically induced transparency and Autler-Townes splitting. This opens up a new dimension in the design of functional elements of photonics and may lead to applications far beyond those that we currently anticipate. Secondly, we wish to show that a bent single mode fiber-based resonator already consists, effectively, of two coupled resonators. This enables one to obtain a full range of Fano-like resonant features without

Manuscript received May 19, 2020; revised July 13, 2020; accepted July 26, 2020. This work was supported by the Russian Foundation for Basic Research under Grant 20-02-00556A. *(Corresponding author: Anton V. Dyshlyuk.)*

Anton V. Dyshlyuk is with the Institute of Automation and Control Processes (IACP) FEB RAS, Far Eastern Federal University (FEFU) and Vladivostok State University of Economics and Service (VSUES), Vladivostok, Russia (e-mail: anton_dys@iacp.dvo.ru).

UlianaA. Eryusheva is on leave from the Institute of Automation and Control Processes (IACP) FEB RAS Vladivostok, Russia (e-mail: muzika.com@inbox.ru).

Oleg B. Vitrik is with the Institute of Automation and Control Processes (IACP) FEB RAS, Far Eastern Federal University (FEFU), Vladivostok, Russia (e-mail: oleg_vitrik@mail.ru).

Color versions of one or more of the figures in this article are available online at https://ieeexplore.ieee.org.

Digital Object Identifier 10.1109/JLT.2020.3021122

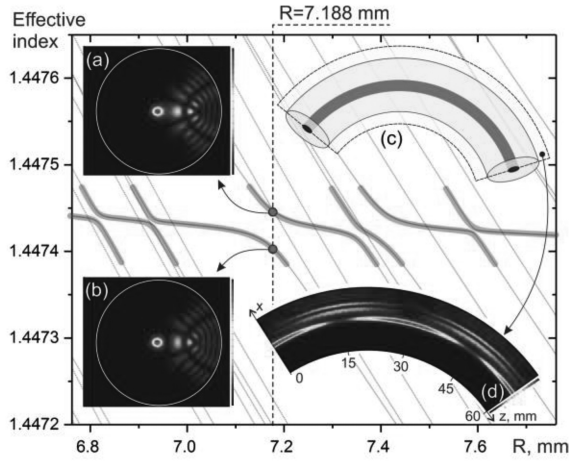

Fig. 1. Effective indexes of the bent single-mode optical fiber supermodes vs. bend radius at a fixed wavelength of 1550 nm. In the insets: (a), (b) amplitude profiles of the two supermodes at the radius of a pronounced anti-crossing of their dispersion curves (R = 7.188 mm), (c) schematic drawing of the bent single-mode optical fiber (shown in pale yellow is the symmetry plane), (d) electric field amplitude distribution of guided light in the longitudinal section of the bent optical fiber at R = 7.188 mm.

the need for designing two separate coupled resonators (such as coupled ring resonators) or using additional scattering elements (such as FBG) to introduce coupling between different resonant states in a single resonator.

The paper is organized as follows. First, based on the analysis of mode coupling in a bent naked single-mode OF, tunable resonance line splitting in the reflection and transmission spectra of a bent Fabry-Perot fiber-optic resonator will be demonstrated, similar to the well-known Autler-Townes splitting. Then, the effect of all major geometric parameters of the bent resonator on the observed splitting will be demonstrated and discussed. In the final part of the article we will present the experimental results, make their comparison with the results of numerical modeling, and discus further research directions.

II. Numerical Results and Discussion

The bent single-mode SMF-28-type optical fiber under study is shown schematically in Fig. 1(c) and has the following parameters: core radius $\rho_1 = 4.15$ μm, core refractive index $n_1 = 1.4504$, optical cladding radius $\rho_2 = 62.5$ μm, cladding refractive index $n_2 = 1.4447$, and bend radius R. To model propagation of guided light in the fiber we use bidirectional eigenmode expansion method implemented in the Lumerical MODE Solutions software. Throughout the simulations we assume that the polymer coatings have been removed from the fiber so that its quartz optical cladding is in contact with air with RI $n_3 = 1$. Therefore, due to the total internal reflection at the cladding | air interface, not only the core, but also the cladding of the fiber possesses pronounced light-guiding properties. Moreover, due to the large discontinuity in refractive index at the cladding | ambient medium interface, the loss of guided light through tunneling out of the bent fiber is negligible (at the bend radii considered in the work), so that all the modes of the fiber, including cladding modes can, to a good approximation, be considered guided modes with zero propagation losses, with their field confined to the fiber. For this reason, to simplify numerical modeling we disregard radiation modes and use reflecting, rather than absorbing, boundary conditions of the type perfect electric conductor (PEC) at the external boundaries of the calculation domain.

Generally speaking, there are two basic lines of reasoning about light propagation through the bent fiber under study [17]. Within the first appoximate approach, its core and cladding are considered separately: the core supports a single fundamental mode (FM), whereas the cladding - a large number of cladding modes. As a result of bending, the field of the cladding modes shifts along the bend radius so that they are guided predominantly by that outer (with respect to the bend) surface of the cladding, which effectively turns them into whispering gallery modes (WGMs). With certain combinations of wavelength and bend radius, the effective refractive indices of FM and a WGM become equal, which leads to the strong coupling between them. The coupled modes then exchange power as they propagate along the fiber, which is observed as periodic redistribution of guided light intensity between the core and the cladding of the fiber (Fig. 1(d)). The period of this exchange depends on the coupling coefficient determined by the overlap integral of the FM and WGM profiles, and decreases with the growth of the latter [17].

In the second more exact approach, the modes of the entire bent fiber viewed as a whole are calculated, which are hereinafter referred to as supermodes. If no coupling takes place between the FM and WGM, the supermodes, in terms of their effective indexes and profiles, do not differ much from the corresponding modes considered separately. However, when such a coupling does occur, the dispersion curves of supermodes, in contrast to those of FM and WGMs, exhibit a characteristic anti-crossing behavior, which is a well-known signature of the strong coupling regime [18]. This is illustrated in Fig. 1, which shows the effective indexes of bent fiber supermodes vs bend radius at a fixed wavelength of 1550 nm. Within an anti-crossing, the amplitude profiles of both supermodes, as Fig. 1a and 1(b) show, are similar and represent a superposition of the separately considered FM (local maximum in the region of the core) and WGM (field distribution in the cladding to the right of the core) profiles, i.e. they result from the hybridization of the latter. The phase profiles of the supermodes, however, are quite different so that the redistribution of guided light intensity between the core and cladding of the bent fiber corresponds to the interference (beating) of the supermodes as they propagate along the bent fiber with constant amplitudes (in contrast to the separately considered FM and WGM whose amplitudes vary as functions of the coordinate along the bent fiber's optical axis as a result of the coupling). The beating period is given by $\lambda / \Delta n$, where Δn is the difference of the effective indexes of the supermodes at the anti-crossing of their dispersion curves, which, in terms of the separately considered FM and WGM, is determined by their coupling coefficient.

The exchange of power between the coupled FM and WGM has a clear parallel to a simple mechanical system of two coupled pendulums (Fig. 2(b)). In the free oscillation regime, the growth

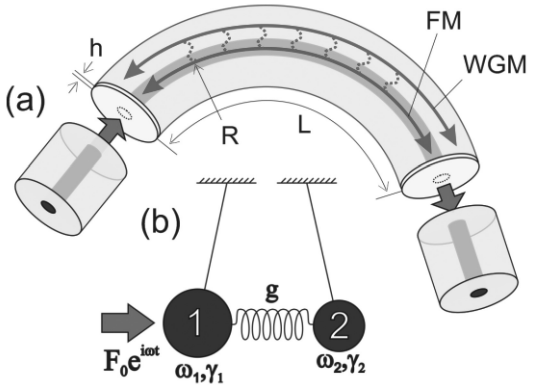

Fig. 2. Schematic of the bent fiber optic Faby-Perot resonator (a) and its mechanical analogy (b)

in oscillation amplitude of one of them is accompanied by the decrease of that of the other [19], i.e. their motion in time is analogous to the spatial variation of the amplitudes of the coupled FM and WGM in the bent fiber (Fig.1(d)).

It is well known that in mechanical systems of coupled oscillators one can readily observe Fano resonances as well as effects similar to the Autler-Townes splitting but in the forced, rather than free, oscillation regime under the action of a harmonic driving force applied to one of the pendulums [7], [18]. At a sufficiently high coupling coefficient the resonance peak in the frequency response of the driven oscillator splits and, depending of the resonant frequency of the other oscillator, one can obtain either symmetric splitting pattern characteristic of the Aulter-Townes effect, or asymmetric splitting with a pronounced dominant peak and weak secondary peak with an asymmetric line shape (insets 1-5 in Fig. 3(a)-(d)).

To realize a similar oscillation regime in the optical domain using a bent single-mode optical fiber let us form a Fabry-Perot resonator (FPR) by applying gold mirrors of thickness h to the end faces of a section of bent fiber of length L as shown in Fig. 2a. Light is fed into and output from the resonator through straight input and output section of the same fiber. Such a resonator can be viewed as two separate coupled resonators corresponding to the longitudinal resonances of the coupled fundamental (FM-resonator) and whispering gallery (WGM-resonator) modes. The excitation light guided by the core of the input fiber section and fed into the core of the bent resonator through the left mirror plays the same role as the driving force applied to one of the pendulums in the mechanical system (Fig. 2(b)).

We plot in Fig. 3 the numerically calculated reflection and transmission spectra of the bent FPR for various bend radii near R = 7.188 mm where a pronounced anti-crossing is observed in the dispersion curves of the supermodes of the bent optical fiber (Fig. 1).

For the sake of comparison, we also show with semi-transparent lines in Fig. 3(c) the reflection and transmission spectra of the corresponding straight resonator. The reflection and transmission coefficients are defined, respectively, as the ratio of powers of the reflected FM in the input fiber section and transmitted FM in the output section to the power supplied by the exciting fundamental mode in the input section.

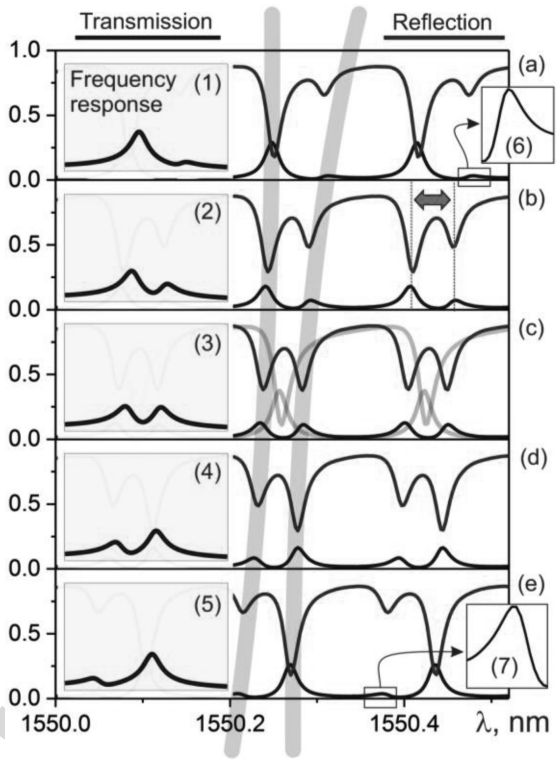

Fig. 3. The calculated reflection and transmission spectra of the bent fiber-optic Fabry-Perot resonator at L = 5mm, h = 10 nm and R = 7.15 mm (a); R = 7.175 mm (b); R = 7.188 mm (c); R = 7.2 mm (d); R = 7.225 (e). In Fig. 3 (c), for comparison, the reflection and transmission spectra of the corresponding straight resonator (L = 5 mm, h = 10 nm) are shown with semi-transparent lines. The insets on the left show the frequency response of the driven pendulum 1 in the mechanical system, calculated for $\omega_1 = 1$, $\gamma_1 = \gamma_2 = 0.1$, g = 0.2, and $\omega_2 = 1.2$ (1) ; $\omega_2 = 1.05$ (2); $\omega_2 = 0.98$ (3); $\omega_2 = 0.9$ (4); $\omega_2 = 0.75$ (5). The insets (6) and (7) show an enlarged view of the secondary peak in the transmission spectrum of the bent FPR with an asymmetric Fano line shape. The gray vertical semi-transparent lines illustrate the shift of the split resonance lines with changing of the bend radius.

As seen from the comparison of the straight and bent RFP spectra in Fig. 3c, the bending of the resonator brings about splitting of the resonances, which at R = 7.188 mm is symmetric and similar to the Autler-Townes splitting. Increasing or decreasing the bend radius relative to R = 7.188 mm shifts the split resonance lines in a manner shown schematically with grey vertical semi-transparent lines. Obviously, the pattern of this shifting is defined by the anti-crossing behavior of the dispersion curves of the bent fiber supermodes (Fig. 1). Furthermore, as the bend radius departs from the resonant value of 7.188 mm the secondary peak in the transmission spectrum and the corresponding dip in the reflection spectrum become less pronounced, which makes the splitting less appreciable.

We also note that at R = 7.15 mm and R = 7.225 mm the weak secondary transmission peak has an asymmetric line shape characteristic of a low Q-factor Fano resonance (insets 6 and 7 in Fig. 3(a), 3(e)).

To interpret the obtained results, it is worthwhile to compare the transmission spectrum of the bent fiber optic resonator with the frequency response of the driven pendulum in the mechanical oscillatory system (insets 1-5 in Fig. 3(a)-(e)). Clearly,

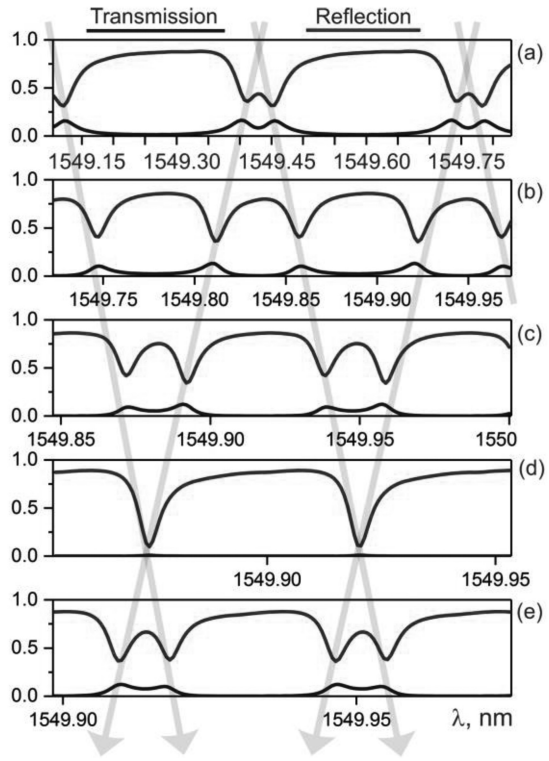

Fig. 4. The calculated transmission and reflection spectra of a bent Fabry-Perot fiber-optic resonator at R = 7.188 mm, h = 10 nm and L = 2.5 mm (a); L = 7.5 mm (b); L = 12.5 mm (c); L = 18 mm (d); L = 22.5 mm (e). The gray vertical lines schematically illustrate the displacement of the split resonance lines as the length of the resonator changes.

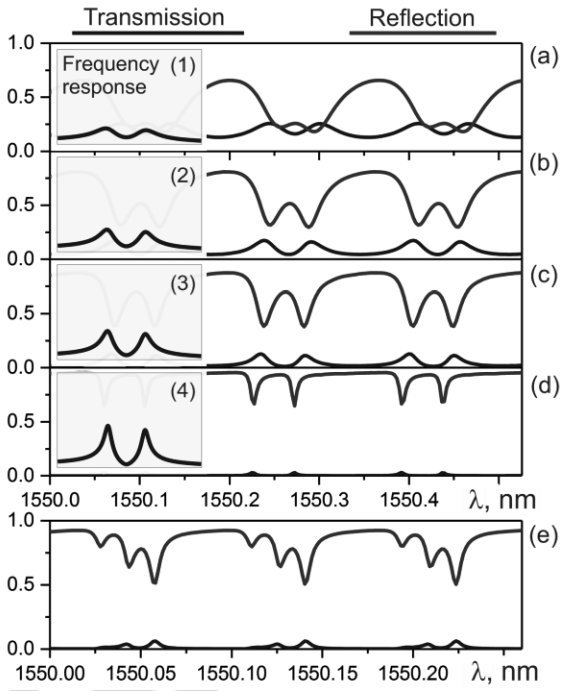

Fig. 5. The calculated transmission and reflection spectra of a bent Fabry-Perot fiber-optic resonator at R = 7.188 mm, L = 5 mm and various mirror thicknesses: h = 5 nm (a); h = 7.5 nm (b); h = 10 nm (c); h = 22.5 nm (d). The insets on the left show the frequency response of the driven pendulum 1 in the mechanical oscillatory system, calculated for $\omega_1 = 1$, $\omega_2 = 0.98$, g = 0.2 and $\gamma_1 = \gamma_2 = 0.15$ (1); 0.1 (2); 0.075 (3); 0.05 (4). Figure (e) shows an example of irregular splitting of the bend FPR resonances when the fundamental mode is coupled simultaneously to two WGMs (R = 7.375 mm, L = 10 mm, h = 15 nm).

these spectra are virtually identical, which is an evidence of a close analogy between the mechanical and optical systems under consideration. In terms of this analogy, the FM-resonator corresponds to the driven pendulum 1, whereas WGM-resonator – to the coupled pendulum 2 (Fig. 2(b)). The coupling between fundamental and whispering gallery modes in the bent fiber then plays the role of the coupling spring in the mechanical system.

As a result of the strong dependence of WGM effective index on the bend radius, the resonances of the WGM-resonator shift with changing R, whereas the resonant frequencies of the FM-resonator remain nearly constant. Changing the bend radius is thus equivalent to varying the second pendulum's resonant frequency (ω_2) while keeping that of the first one (ω_1) fixed in the mechanical system. R = 7.188 mm corresponds to the phase matching condition between FM and WGM in the bent fiber, which makes the resonant frequencies of the FM- and WGM-resonators match each other. This case, therefore, corresponds to $\omega_1 \approx \omega_2$ in the mechanical system when a clear-cut symmetric resonance splitting is observed. As the bend radius departs from 7,188 mm the phase matching between FM and WGM is gradually lost making the splitting asymmetric and less pronounced, which in terms of the mechanical system corresponds to $\omega_1 \lessgtr \omega_2$.

To demonstrate the effect of the FPR length on the resonance splitting, we plot in Fig. 4 its transmission and reflection spectra calculated at L = 2.5 …22.5 mm, R = 7.188 mm, and h = 10 nm. As seen from the figure, increasing the length of the resonator makes the splitting look more pronounced by driving the split resonance lines further apart. This, however, is an apparent effect arising from different scales on the horizontal axes of Fig. 4(a)-(e). A closer analysis of the presented spectra shows that an increase in the length of the resonator makes its lines sharper and more closely spaced while the splitting remains unchanged in its absolute value.

An interesting feature is observed at L = 18 mm (Fig. 4(d)) when the resonant transmission is almost zeroed by the overlap of the split lines from two adjacent resonances, which is accompanied by a deep minimum in the reflection spectrum. The calculation of the intensity distribution in the bent resonator shows that almost all of the injected power goes, in this case, into the cladding of the output fiber section.

Figure 5 illustrates the effect of the mirror thickness on the resonance splitting of the bent FPR by showing its transmission and reflection spectra calculated at h = 5; 7.5; 10 and 22.5 nm; R = 7.188 mm, L = 5 mm. As seen from the graphs, the primary effect of thicker mirrors is to make the resonance lines sharper as a result of higher mirror reflectivity and, therefore, higher Q-factor of the resonator. Narrowing of the resonance lines, in turn, makes their splitting more clear-cut. Disregarding the lowering of the resonant transmission with an increase in *h*, which results from higher absorption losses in thicker mirrors, the calculated transmission spectra, as seen from insets 1-4, are

very similar to the frequency response of the driven pendulum in the mechanical system (Fig. 2(b)) with simultaneously decreasing both pendulums' damping constants γ_1 and γ_2.

All the results shown above are obtained for the bend radii near the resonant value of R = 7.188 mm, which corresponds to the strong coupling of the fundamental mode of the core to one of the cladding whispering gallery modes. There are, however, a great number of such cladding modes many of which can couple to FM at various R values, as can be readily appreciated from Fig. 1. The splitting of resonances similar to that already demonstrated can therefore be observed at different bend radii. Its width is defined by the effective index difference of the hybrid supermodes of the bent fiber at the anti-crossing of their dispersion curves, Δn.

In terms of the separately considered FM and WGM, Δn is determined by their coupling coefficient and is therefore a measure of the coupling strength of FM- and WFM-resonators. As seen from Fig. 1, in the bend radius range from 6.8 to 7.7 mm Δn is largest for the anti-crossing centered at R = 7.188 mm. At the bend radii of other anti-crossings, the width of the splitting will be less, meaning that larger Q-factors of the resonator are required to observe it clearly.

We also note that around certain bend radii the fundamental mode may become coupled to two WGMs simultaneously (Fig. 1). This leads to a more complicated and irregular splitting pattern in the transmission and reflection spectra of the bent FPR, as exemplified by Fig. 5(e).

All the simulation results in this article are obtained for the case when the FM in the input fiber section is polarized linearly in the plane of the fiber bend, which corresponds to the symmetric boundary condition on the symmetry plane of the structure under study (Fig. 1(c)). Calculations for the orthogonal polarization yield similar results albeit slightly shifted in wavelength due to the polarization dependence of WGMs effective indexes.

III. Experiment

A schematic of the experimental setup for the study of the resonance splitting of the bent fiber optic Fabry-Perot resonator, along with the experimental results are shown in Fig. 6.To measure experimentally the reflection spectra of the bent fiber optic Fabry-Perot resonator we prepared several samples of such resonators of 1 cm-long sections of an SMF-28-type telecom optical fiber. The end faces of the resonators are coated with a thin layer of gold by the electron beam evaporation technique in the ADVAVAC vacuum chamber. We then fix the resonators upon rounded support 7 (Fig. 6(a)) and lead-in fiber 3 is aligned with the input end of the resonator using optical microscopes, broadband light source 1 (Thorlabs ASE730) and optical spectrum analyzer 8 (Yokogawa AQ6370B). After alignment the contact point is secured with epoxy adhesive 4. Excitation of the resonator and the measurement of its reflection spectrum is carried out via fiber optic circulator 2.

The resonator is bent by calibrated displacement of its loose end using a precision translation stage 6. The evolution of the bent resonator's measured reflection spectrum with varying bend radius is illustrated in Fig. 6(b)-(f). The insets 1-5 of these figures show the corresponding simulation results. Obviously,

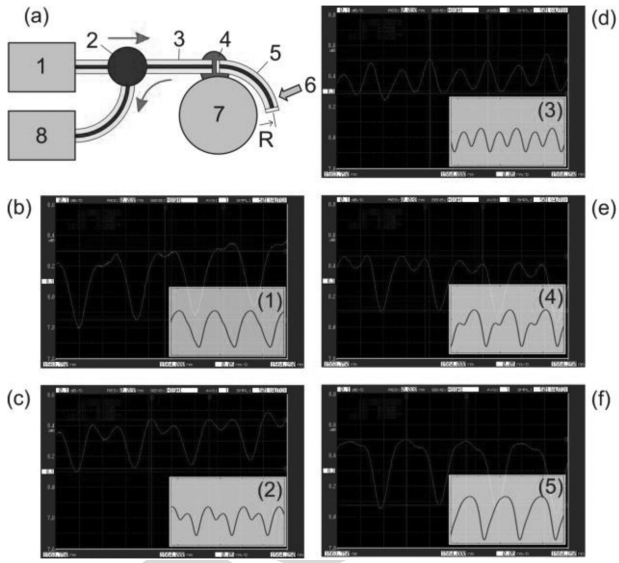

Fig. 6. Schematic representation of the experimental setup for studying the reflection spectrum of a bent fiber optic Fabry-Perot resonator (a): 1 - broadband light source (Thorlabs ASE 730), 2 - fiber-optic circulator , 3 – exciting optical fiber, 4 - fixing the contact point with an epoxy adhesive, 5 – bent fiber optic Fabry-Perot resonator, 6 - bending the resonator by calibrated displacement of its loose end using a precision translation stage , 7 – a rounded support, 8 - optical spectrum analyzer (Yokogawa AQ6370B). The evolution of the measured reflection spectra with varying bend radius (b)-(f). Yellow insets (1-5) show the corresponding numerically calculated reflection spectra at L = 1 cm, h = 5 nm and R = 7.375 mm (1), R = 7.4 mm (2), R = 7.425 mm (3), R = 7.45 mm (4), R = 7.475 mm (5).

the experimental and numerical results are in good agreement, which confirms the validity of the numerical modeling carried out in this work.

IV. Conclusions

We have, thus, studied tunable splitting of resonances in the transmission and reflection spectra of the bent single mode optical fiber-based Fabry-Perot resonator, which is similar to the well-knows Autler-Townes splitting. The splitting is shown to result from the strong coupling between the fundamental mode of the core and whispering gallery modes of the cladding of the bent fiber. We have demonstrated and discussed how the splitting is affected by all major parameters of the resonator. The validity of the numerical modeling is confirmed by the experimental results.

We must note that the resonance splitting demonstrated in this work does not lead to narrow spectral features and sharp drops in the transmission and reflection spectra, characteristic of high Q-factor Fano resonances and electromagnetically induced transparency. This is due to the fact that the latter effects arise from the interference of a narrow resonant lineshape with a nonresonant continuum or another low Q-factor resonance. In particular, to observe such effects in the mechanical system of two coupled pendulums (Fig. 2(b)) the following condition must be satisfied: $\gamma_2 << \gamma_1$ [7]. In the studied case of coupling between FM- and WGM-resonators, however, their losses, defined primarily by the transmission through the input and output mirrors, are equal. To enable high Q-factor Fano

resonance and electromagnetically induced transparency-like operation regimes in the bent fiber optic Fabry-Perot resonator, which are more attractive in terms of the development fiber optic sensing and switching devices, variable transmission mirrors must be employed providing low losses for the WGM-resonator and high losses for the FM-resonator. The simplest example of such a mirror is a thick gold layer on the fiber end face with a hole at the center produced by a laser ablation technique. Results of further researches in this direction will be published elsewhere.

We stress again that although we have studied here the Fabry-Perot resonator, the particular type of resonator is not essential and similar results can be obtained with other kinds of bent fiber-based resonators. The most important point we wish to make is that, by introducing a longitudinal resonator, one can obtain a full range of Fano-like resonant features with a single section of conventional bent single-mode optical fiber without resorting to any additional coupling elements or building a system of two separate coupled resonators. This opens up a new degree of freedom in the design of functional elements of photonics based on bent optical fibers and waveguides and may lead to diverse applications far beyond what we currently anticipate.

REFERENCES

[1] U. Fano, "Sullo spettro di assorbimento dei gas nobili presso il limite dello spettro darco," *Il Nuovo Cimento*, vol. 12, pp. 154–161, 1935.

[2] U. Fano, "Effects of configuration interaction on intensities and phase shifts," *Phys. Rev.*, vol. 124, no. 6, 1961, Art. no. 1866.

[3] M. F. Limonov *et al.*, "Fano resonances in photonics," *Nature Photon.*, vol. 11, no. 9, 2017, Art. no. 543.

[4] B. Luk'yanchuk *et al.*, "The Fano resonance in plasmonic nanostructures and metamaterials, *Nature Mater.*, vol. 9, no. 9, 2010, Art. no. 707.

[5] A. E. Miroshnichenko, S. Flach, and Y. S. Kivshar, "Fano resonances in nanoscale structures," *Rev. Modern Phys.*, vol. 82, no. 3, 2010, Art. no. 2257.

[6] M. Rahmani, B. Luk'yanchuk, and M. Hong, "Fano resonance in novel plasmonic nanostructures," *Laser Photon. Rev.*, vol. 7, no. 3, pp. 329–349, 2013.

[7] C. L. Garrido Alzar, M. A. G. Martinez, and P. Nussenzveig, "Classical analog of electromagnetically induced transparency," *Amer. J. Phys.*, vol. 70, no. 1, pp. 37–41, 2002.

[8] A. V. Dyshlyuk, "Tunable Fano-like resonances in a bent single-mode waveguide-based Fabry–Perot resonator," *Opt. Lett.*, vol. 44, no. 2, pp. 231–234, 2019.

[9] А. В. Дышлюк, "Демонстрация резонансных эффектов типа расщепления Аутлера–Таунса, электромагнитно-индуцированной прозрачности и резонансов Фано в деформированном волноводном резонаторе," *Компьютерная оптика*, vol. 43, no. 1, 2019.

[10] A. V. Dyshlyuk *et al.*, "Numerical and experimental investigation of surface plasmon resonance excitation using whispering gallery modes in bent metal-clad single-mode optical fiber," *J. Lightw. Technol.*, vol. 35, no. 24, pp. 5425–5431, 2017.

[11] P. Wang *et al.*, "Macrobending single-mode fiber-based refractometer," *Appl. Opt.*, vol. 48, no. 31, pp. 6044–6049, 2009.

[12] P. Wang *et al.*, "A macrobending singlemode fiber refractive index sensor for low refractive index liquids," *Photon. Lett. Poland*, vol. 2, no. 2, pp. 67–69, 2010.

[13] Y. N. Kulchin, O. B. Vitrik, and S. O. Gurbatov, "Effect of small variations in the refractive index of the ambient medium on the spectrum of a bent fibre-optic Fabry–Perot interferometer," *Quantum Electron.*, vol. 41, no. 9, 2011, Art. no. 821.

[14] Y. Xu *et al.*, "Optical refractive index sensors with plasmonic and photonic structures: Promising and inconvenient truth," *Adv. Opt. Mater.*, vol. 7, no. 9, 2019, Art. no. 1801433.

[15] E. Kretschmann and H. Raether, "Radiative decay of non radiative surface plasmons excited by light," *Zeitschrift für Naturforschung A*, vol. 23, no. 12, pp. 2135–2136, 1968.

[16] J. Homola, *Surface Plasmon Resonance Based Sensors Berlin*. Berlin, Germany: Springer, 2006.

[17] A. W. Snyder and J. Love, *Optical waveguide theory*. Berlin, Germany: Springer Science & Business Media, 2012.

[18] L. Novotny, "Strong coupling, energy splitting, and level crossings: A classical perspective," *Amer. J. Phys.*, vol. 78, no. 11, pp. 1199–1202, 2010.

[19] V. Picciarelli and R. Stella, "Coupled pendulums: A physical system for laboratory investigations at upper secondary school," *Phys. Educ.*, vol. 45, no. 4, 2010, Art. no. 402.

Anton V. Dyshlyuk received the Ph.D. degree from Far Eastern State Technical University (FEFU), Vladivostok, Russia, in 2003, majoring in radio communications, radio broadcasting, and television. He is currently a Senior Researcher with the Institute of Automation and Control Processes of FEB RAS as well as with FEFU and Vladivostok State University of Economics and Service (VSUES), Vladivostok, as a Lecturer. His research interests include fiber optics, quantum electronics, fiber optic sensors and measuring systems, biosensing, plasmonics, and nanophotonics.

Uliana A. Eryusheva received the graduate degree from the Vladivostok State University of Economics and Service, Vladivostok, Russia, in 2017 and the master's degree from Far Eastern Federal University, Vladivostok, Russia, in 2019. Her research interests include fiber optics, plasmonics, fiber optic sensors and measuring systems, and bio- and chemosensing.

Oleg B. Vitrik received the graduate degree from Moscow Engineering Physics Institute, Moscow, Russia, in 1986, majoring in solid state physics. He is currently a Principal Researcher with the Institute of Automation and Control Processes of FEB RAS and a Professor of the Far Eastern Federal University, Vladivostok, Russia. His research interests include nano-optics, plasmonics, fiber optics, fiber optic sensors, and measuring systems.